CHAPTER IV

Effect of Hall Current on Heat and Mass Transfer of Free Convective Flow over a Flat Porous Plate Embedded in a Porous Medium

4.1. Introduction

In recent years, the study of heat and mass transfer of free convective MHD flow plays a vital role in many engineering fields due to its applications in various areas such as heat exchanger, petroleum reservoirs, geothermal and geophysical engineering, aerodynamic engineering and others.

In Fluid dynamics, Hall current attains widespread interest due to its applications in many geophysical and astrophysical situations as well as in engineering problems such as Hall accelerators, Hall effect sensors, constructions of turbines and centrifugal machines. MHD flows with Hall current effects are encountered in power generators, MHD accelerators, refrigeration coils, electrical transformers and in flight magneto hydrodynamics.

The study of magneto hydrodynamic flows, heat and mass transfer with Hall currents has an important bearing in engineering applications. Study of effects of Hall currents on flows have been done by many researchers. Anjalidevi and Kayalvizhi (2013) studied nonlinear hydromagnetic flow with radiation and heat source over a stretching surface with prescribed heat and mass flux embedded in a porous medium.

Crane (1970) studied steady boundary layer flow caused by a stretching sheet whose velocity varies linearly with the distance from a fixed point in the sheet. Hall effects on hydromagnetic flow was studied by Pop and Soundalgekar (1974). Gupta and Gupta (1977) studied heat and mass transfer on a stretching sheet with suction or blowing. Shampa Ghosh (2015) studied magneto hydrodynamic boundary layer flow over a stretching sheet with chemical reaction.

Katagiri (1969) investigated the effect of Hall current on the steady boundary layer flow in the presence of a transverse magnetic field. Hossain and Rashid (1987) studied the effect of Hall current on the unsteady free convection flow of a viscous incompressible and electrically conducting fluid, in the presence of foreign gases (such as H_2, CO_2 , H_2O, NH_3) along an infinite vertical porous flat plate in the presence of a uniform transverse magnetic field. Soundalgekar and Uplekar (1986) studied the effect of Hall current in MHD Couette flow with heat transfer. Attia

(1998) studied Hall current effects on the velocity and temperature fields on an unsteady Hartmann flow using perturbation techniques.

The absence of Hall current in Shampa Ghosh (2015) motivated us to take up the present work wherein we study the effect of Hall current on heat and mass transfer in a steady free-convective flow in the presence of a uniform transverse magnetic field in a porous medium. The governing equations are transformed by a similarity transformation into a system of non-linear ordinary differential equations which are solved numerically by fourth order Runge-Kutta Method. Numerical calculations are performed for various values of the magnetic parameter, Hall current parameter, Schimdt number and Soret number. The results are given for the coefficients of skin-friction, rate of heat transfer and rate of mass transfer for various values of magnetic and Hall current parameters.

4.2. Flow Description and Governing Equations

We consider a steady free-convective flow of an incompressible viscous electrically conducting fluid over a porous flat plate in the presence of a transverse magnetic field and Hall current embedded in porous medium. We introduce a stationary frame of reference (x, y, z) such that x-axis is taken along the direction of motion, y-axis is normal to the surface and z-axis is normal to the xy-plane (see figure 4.1). A uniform magnetic field $\vec{B}_0$ is imposed along y-axis and the effect of Hall current is taken into account. The temperature and the concentration are maintained at prescribed constant values T_w, C_w at the plate and T_∞ ,C_∞ are the fixed values far away from the plate.

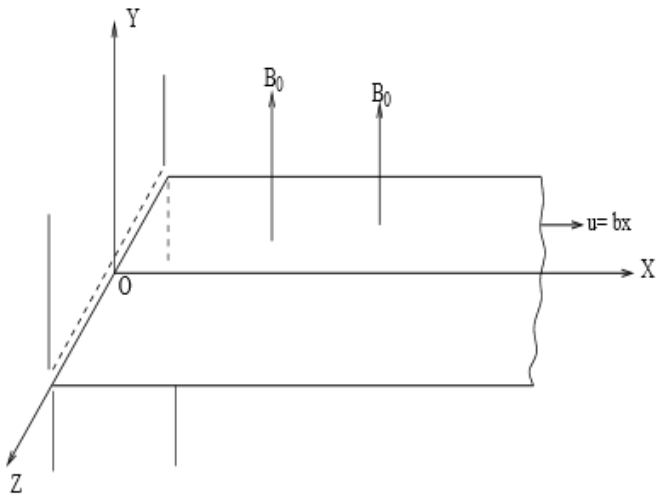

Fig 4.1 Schematic diagram of the problem

Taking Hall effects into account the generalized Ohm's law is taken in the following form,

$$\vec{J} = \frac{\sigma}{1+m^2}\left(\vec{E} + \vec{V} \times \vec{B} - \frac{1}{en_e}\vec{J} \times \vec{B}\right)$$

in which $\vec{V}, \vec{E}, \vec{B}, \vec{J}, m = \frac{\sigma B_0}{en_e}, \sigma, e$ and n_e represent the velocity vector, intensity vector of the electric field, magnetic vector, electric current density vector, Hall parameter, electrical conductivity, charge of the electron and number density of the electron. The effect of Hall current gives rise to a force in the z-direction which in turn produces a cross flow velocity in this direction.

In the present work, the following assumptions are made:

- Flow of a Newtonian and electrically conducting fluid is considered which is steady, viscous, incompressible and laminar in nature.
- Due to the existence of charged particles in the fluidic domain, Hall Effect is observed in presence of an external magnetic field.
- A uniform magnetic field $\vec{B}_0$ is assumed unaltered in the positive y-direction.
- Boussinesq approximation is employed.
- Viscous dissipation and heat source are neglected.
- Thermo diffusion effects are considered.

Due to the above assumptions, the free-convection flow along with heat and mass transfer and generalized Ohm's law with Hall current effect are governed by the following system of equations:

$$\frac{\partial u}{\partial x} + \frac{\partial v}{\partial y} = 0 \tag{4.1}$$

$$u\frac{\partial u}{\partial x} + v\frac{\partial u}{\partial y} = \gamma\frac{\partial^2 u}{\partial y^2} + g\beta(T - T_\infty) + g\beta^*(C - C_\infty) - \frac{\sigma B_0^2}{\rho(1+m^2)}(u + mw) - \frac{\gamma}{k}u \tag{4.2}$$

$$u\frac{\partial w}{\partial x} + v\frac{\partial w}{\partial y} = \gamma\frac{\partial^2 w}{\partial y^2} + \frac{\sigma B_0^2}{\rho(1+m^2)}(mu - w) - \frac{\gamma}{k}w \tag{4.3}$$

$$u\frac{\partial T}{\partial x} + v\frac{\partial T}{\partial y} = \frac{\kappa}{\rho C_p}\frac{\partial^2 T}{\partial y^2} \tag{4.4}$$

$$u\frac{\partial C}{\partial x} + v\frac{\partial C}{\partial y} = D_M\frac{\partial^2 C}{\partial y^2} + D_T\frac{\partial^2 T}{\partial y^2} \tag{4.5}$$

In the above system of equations, (u, v, w) are the velocity components along the (x, y, z) directions respectively, g is the acceleration due to gravity, β is the coefficient of thermal expansion, β^* is the coefficient of expansion with concentration, T, C, μ, ρ, σ and $\gamma = (\mu/\rho)$ represent respectively the temperature,

mass concentration, coefficient of viscosity, density, electrical conductivity and kinematic viscosity of the fluid. The constant parameters in the system: $k, C_p, \kappa,\ D_M$ and D_T represent respectively the permeability of porous material, specific heat at constant pressure, thermal conductivity of the fluid, molecular diffusivity and thermal diffusivity.

The appropriate boundary conditions for the velocity, temperature and mass concentration are given by,

$u = bx, \quad v = 0,\ w = 0$ at y=0; $\quad u = w = 0 \quad$ as $\ y \to \infty,$ (4.6)

$T = T_w \qquad$ at $\ y = 0;\ \ T \to T_\infty$ as $y \to \infty$, (4.7)

$C = C_w \qquad$ at $\ y = 0;\ \ C \to C_\infty$ as $y \to \infty$, (4.8)

where b > 0 being stretching rate of the sheet.

4.3. Solution of the Problem

In this work similarity technique is employed to solve the system of equations (4.1)-(4.5) along with the boundary conditions (4.6)-(4.8). The similarity transformations are,

$$\left.\begin{aligned} u = bxf'(\eta),\ v = -\sqrt{b\gamma}f(\eta),\ w = bxg(\eta),\ \eta = \sqrt{\frac{b}{\gamma}}\,y, \\ \theta(\eta) = \frac{T-T_\infty}{T_w-T_\infty}, \qquad \phi(\eta) = \frac{C-C_\infty}{(C_w-C_\infty)} \end{aligned}\right\} \tag{4.9}$$

Introducing the above transformations in equations (4.1)-(4.5), we obtain the system of ordinary differential equations,

$$f''' + ff'' - f'^2 + Gr\theta + Gc\phi - \frac{M}{1+m^2}(f' + mg) - k^* f' = 0, \tag{4.10}$$

$$g'' + fg' - \left(f' + \frac{M}{1+m^2} + k^*\right)g + \frac{Mm}{1+m^2}f' = 0, \tag{4.11}$$

$$\theta'' + Prf\theta' = 0, \tag{4.12}$$

$$\phi'' + Scf\phi' + ScSr\theta'' = 0. \tag{4.13}$$

where $M = \frac{\sigma B_0^2}{\rho b}$ is the magnetic parameter, $Gr = \frac{g\beta(T_w-T_\infty)}{b^2 x}$ is the Local Grashof number, $Gc = \frac{g\beta^*(C_w-C_\infty)}{b^2 x}$ is the local modified Grashof number, $m = \frac{\sigma B_0}{en_e}$ is the Hall current parameter, $Pr = \mu C_p/\kappa$ is the Prandtl number, $Sc = \frac{\gamma}{D_m}$ is the Schmidt number, $Sr = \frac{(T_w-T_\infty)D_T}{(C_w-C_\infty)\gamma}$ is the Soret number, $k^* = 1/Da_x Re_x$ is the permeability of porous medium and $Da_x = k/a^2 = k_0/x$ is the local Darcy number. Here k_0 is the constant, $Re_x = \frac{bx^2}{\gamma}$ is the Reynolds number

The boundary conditions (4.6)-(4.8) transform to the following form,

$f(\eta) = 0, \quad f'(\eta) = 1 \text{ at } \eta = 0; \quad f'(\eta) \to 0 \text{ as } \eta \to \infty$ (4.14)

$g(\eta) = 0 \text{ at } \eta = 0; \qquad g(\eta) \to 0 \text{ as } \eta \to \infty$ (4.15)

$\theta(\eta) = 1 \text{ at } \eta = 0; \qquad \theta(\eta) \to 0 \text{ as } \eta \to \infty$ (4.16)

$\phi(\eta) = 1 \quad \text{at } \eta = 0; \qquad \phi(\eta) \to 0 \text{ as } \eta \to \infty$ (4.17)

The non-linear coupled ordinary differential equations (4.10)-(4.13) subject to boundary conditions (4.14)-(4.17) are solved numerically using shooting method with fourth order Runge-Kutta method.

$f' = w, \ w' = v, \ \theta = y, \ \theta' = z, \ \phi = b, \ \phi' = e \ , g = i, g' = a.$

$v' = -fv + w^2 - Gry - Gcb + \frac{M}{1+m^2}(w + mi) + k^* w,$ (4.18)

$a' = -fa + \left(w + \frac{M}{1+m^2} + k^*\right) i - \frac{Mm}{1+m^2} w$ (4.19)

$z' = -Prfz,$ (4.20)

$e' = -Scfe - ScSrz'$ (4.21)

and boundary conditions become,

$f(0) = 0, \ w(0) = 1, \ i(0) = 0, \quad y(0) = 1, \ \ b(0) = 1 \text{ at } \eta = 0$ (4.22)

$w(0) \to 0, a(0) \to 0, y(0) \to 0, \ b(0) \to 0 \text{ as } \eta \to \infty$ (4.23)

We have solved the equations (4.18)-(4.21) with boundary conditions (4.22) and (4.23) using shooting method.

The major physical quantities of engineering interest the skin-friction coefficient C_f , the local Nusselt number Nu_x, and the local Sherwood number Sh_x are defined respectively as follows,

Skin-friction co-efficient:

$C_{fx} = \frac{\tau_x}{\mu bx\sqrt{\frac{b}{\gamma}}}$, Here Shear stress along x-direction

$C_{fz} = \frac{\tau_z}{\mu bx\sqrt{\frac{b}{\gamma}}}$, Here Shear stress along z-direction (4.24)

Local Nusselt number: $Nu_x = \frac{q_w}{k\sqrt{\frac{b}{\gamma}}(T_w - T_\infty)}$ (4.25)

Local Sherwood number: $Sh_x = \frac{m_w}{D\sqrt{\frac{b}{\gamma}}(C_w - C_\infty)}$ (4.26)

where τ_x and $\tau_z$is the skin-friction along x and z- direction respectively, q_w is the heat flux and m_w is the mass flux at the surface.

$\tau_x = \mu\left(\frac{\partial u}{\partial y}\right)_{y=0} = \mu bx\sqrt{\frac{b}{\gamma}} f''(0)$

$$\tau_z = \mu \left(\frac{\partial w}{\partial y}\right)_{y=0} = \mu bx \sqrt{\frac{b}{\gamma}}\, g'(0) \tag{4.27}$$

$$q_w = -k \left(\frac{\partial T}{\partial y}\right)_{y=0} = -k \sqrt{\frac{b}{\gamma}}\, (T_w - T_\infty)\theta'(0) \tag{4.28}$$

$$m_w = -D \left(\frac{\partial C}{\partial y}\right)_{y=0} = -D \sqrt{\frac{b}{\gamma}}\, (C_w - C_\infty)\phi'(0) \tag{4.29}$$

Substituting equations (4.27), (4.28) and (4.29) into the equations (4.24), (4.25) and (4.26) we get

$$f''(0) = C_{fx}$$

$$g'(0) = C_{fz}$$

$$-\theta'(0) = Nu_x$$

$$-\phi'(0) = Sh_x$$

4.4. Results and Discussion

Numerical computations are performed for several values of dimensionless parameters involved in the equations such as magnetic parameter M, Hall current parameter m, Schmidt number Sc, Soret number Sr. In order to examine the computed results and understand the behaviour of various physical parameters of the flows, graphs are plotted. The results of the hydrodynamic characteristics are represented by the velocity, temperature, heat transfer, concentration and mass transfer contours.

Figures (4.2)-(4.4) show the velocity profiles $f'(\eta), f(\eta)$ and $g(\eta)$ corresponding to the axial velocity, transverse velocity and the cross flow velocity for various values of the magnetic parameter M. These figures indicate that the velocity decreases with the increase in the magnetic parameter M. Lorentz force opposes the flow and leads to deceleration of the fluid motion. The cross flow velocity is found to decrease with increasing magnetic parameter M. Figures (4.5) and (4.6) illustrate that the temperature and concentration profiles increase with the increase of magnetic parameter M.

From figures (4.7) and (4.8) it is evident that axial and transverse velocities increase with the increase in the Hall current parameter m. Figure (4.9) shows that for a particular or fixed value of m, $g(\eta)$ attains a maximum value at a certain height η and cross flow velocity $g(\eta)$ decreases gradually in asymptotic nature.

Figures (4.10) and (4.11) illustrate the temperature $\theta(\eta)$ and concentration $\phi(\eta)$ profiles for various values of Hall current parameter m. These two graphs

illustrate that temperature and concentration profiles decrease with increase in Hall current parameter m.

Figures (4.12)-(4.19) depict that the velocity components and concentration profiles decrease with increase in Schmidt number Sc while Soret number has an adverse effect on these profiles i.e., increase in Soret number increase the velocity components and concentration profiles.

From Figures (4.20)–(4.23) we can infer that skin-friction increases due to increase of Hall current parameter m and decreases with increasing magnetic parameter M. The rate of heat transfer $\theta'(0)$ and the rate of mass transfer $\phi'(0)$ decrease, with increase in Hall current parameter m while increase in the magnetic parameter increases the heat and mass flux.

4.5. Conclusion

In this chapter we have investigated the effect of Hall current on free-convective flow along with heat and mass transfer of a viscous, incompressible and electrically conducting fluid over a flat porous plate. The non-linear governing equations together with the boundary conditions are reduced to a system of non-linear ordinary differential equations by using similarity transformations. The system of non-linear ordinary differential equations is solved with shooting procedure using fourth order Runge-Kutta method.

In this study the following conclusions are set out:

- The velocity profiles f', f, g decrease with increase in magnetic parameter M.
- Temperature and concentration profiles increase with the increase in magnetic parameter M.
- The velocity profiles f', f increase with increase in Hall current m, in the case of temperature and concentration a reversal trend is observed.
- Velocity components and concentration profiles decrease with increase in the Schmidt number Sc.
- Due to increase in Soret number velocity components and concentration profiles increase.
- Skin-friction increases due to increase of Hall current parameter m, and decreases with increasing magnetic parameter M.

- The rate of heat transfer $\theta'(0)$ and the rate of mass transfer $\phi'(0)$ decrease, with increase in Hall current parameter m while increase in the magnetic parameter increases the heat and mass flux.

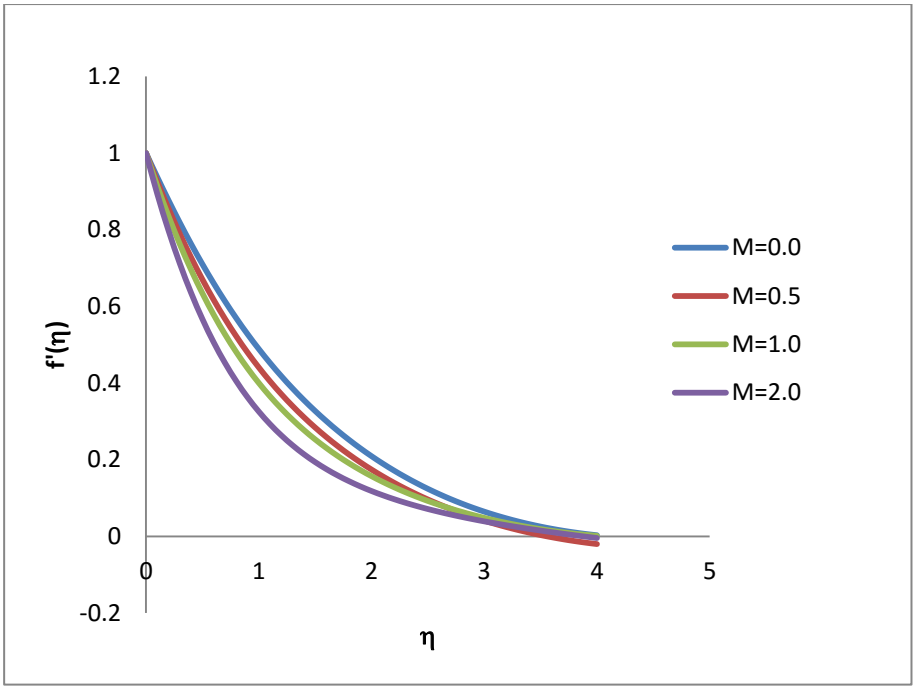

Fig 4.2 Axial velocity of $f'(\eta)$ for various values of magnetic parameter M; Pr=7.0; Sc=0.5; Sr=0.5; Gr=0.5; Gc=0.5; k=0.2; m=1.0*

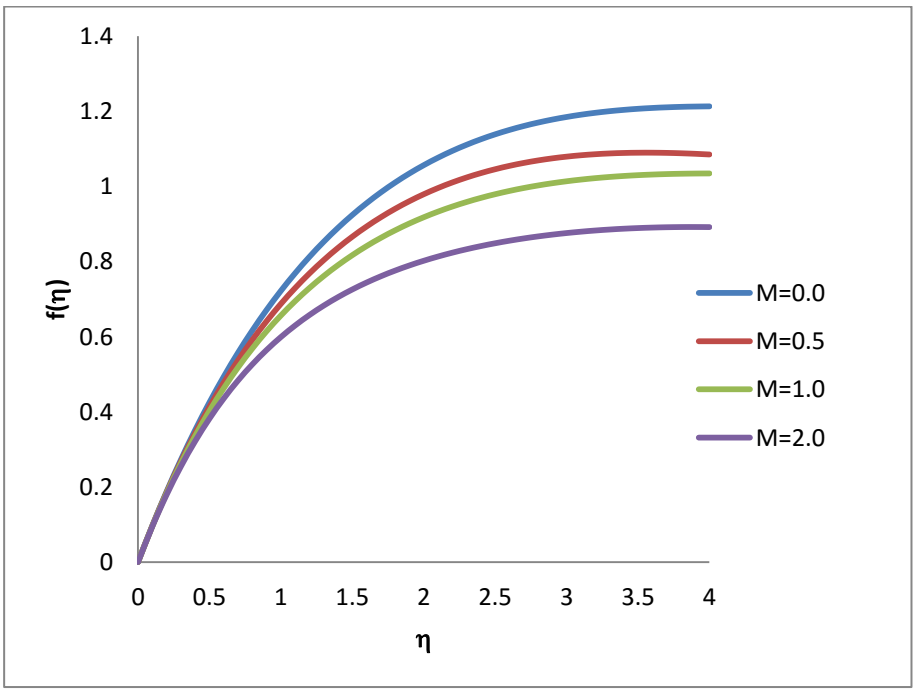

Fig 4.3 Transverse velocity of $f(\eta)$ for various values of magnetic parameter M; Pr=7.0; Sc=0.5; Sr=0.5; Gr=0.5; Gc=0.5; k=0.2; m=1.0*

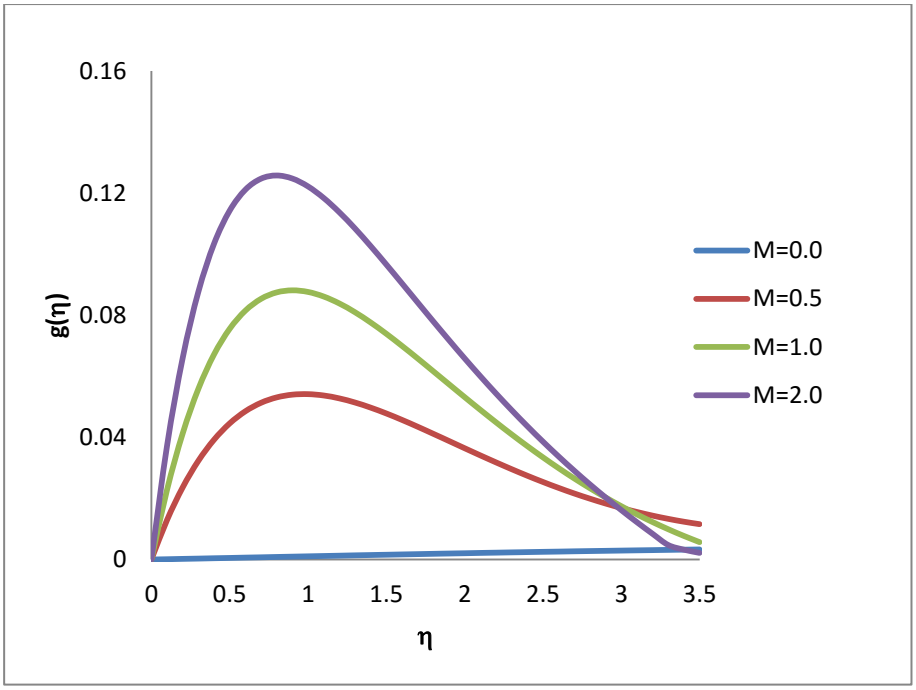

Fig 4.4 Cross flow velocity of $g(\eta)$ for various values of magnetic parameter M; Pr=7.0; Sc=0.5; Sr=0.5; Gr=0.5; Gc=0.5; k=0.2; m=1.0*

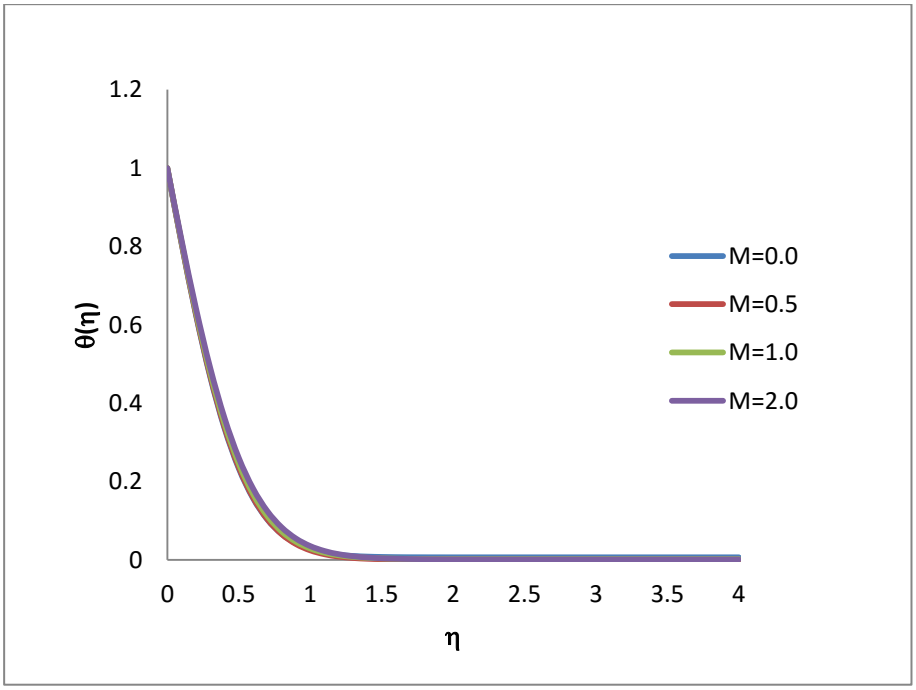

Fig 4.5 Temperature profiles of $\theta(\eta)$ for various values of magnetic parameter M; Pr=7.0; Sc=0.5; Sr=0.5; Gr=0.5; Gc=0.5; k=0.2; m=1.0*

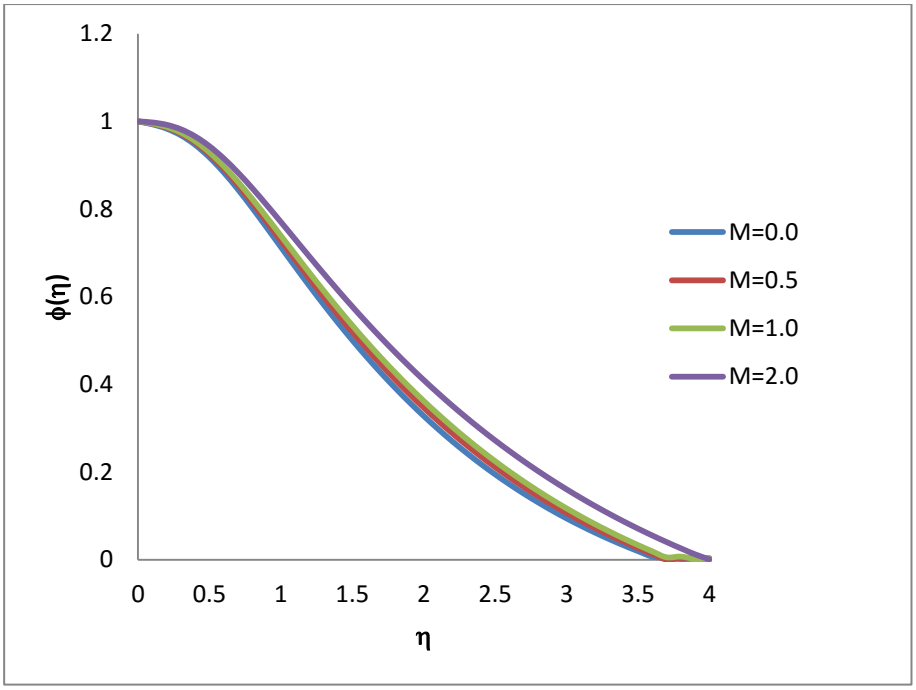

Fig 4.6 Concentration profiles $\phi(\eta)$ for various values of magnetic parameter M; Pr=7.0; Sc=0.5; Sr=0.5; Gr=0.5; Gc=0.5; k=0.2; m=1.0*

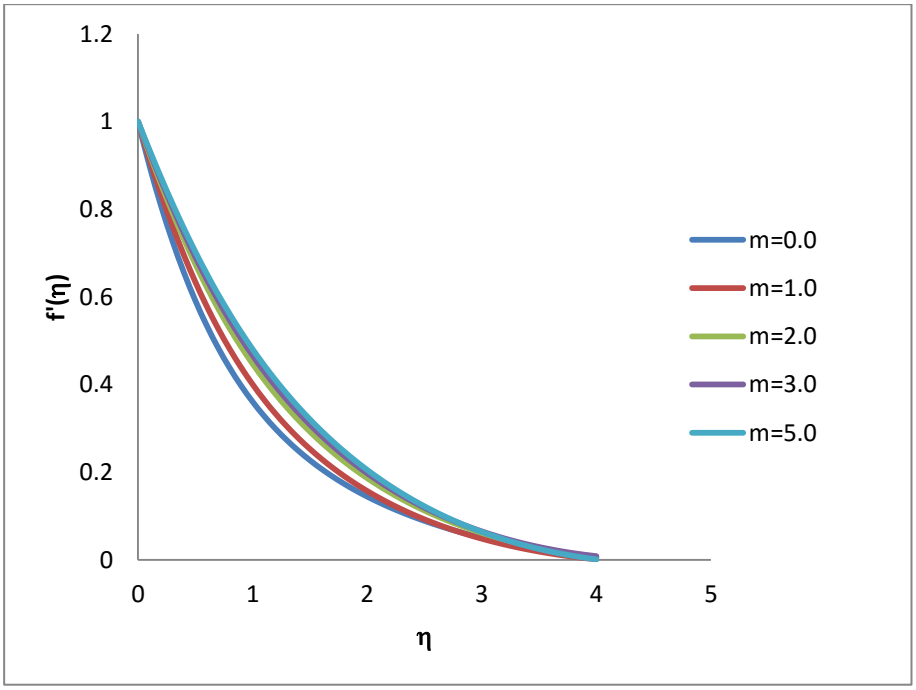

Fig 4.7 Axial velocity of $f'(\eta)$ for various values of Hall Current parameter m; Pr=7.0; Sc=0.5; Sr=0.5; Gr=0.5; Gc=0.5; k=0.2; M=1.0*

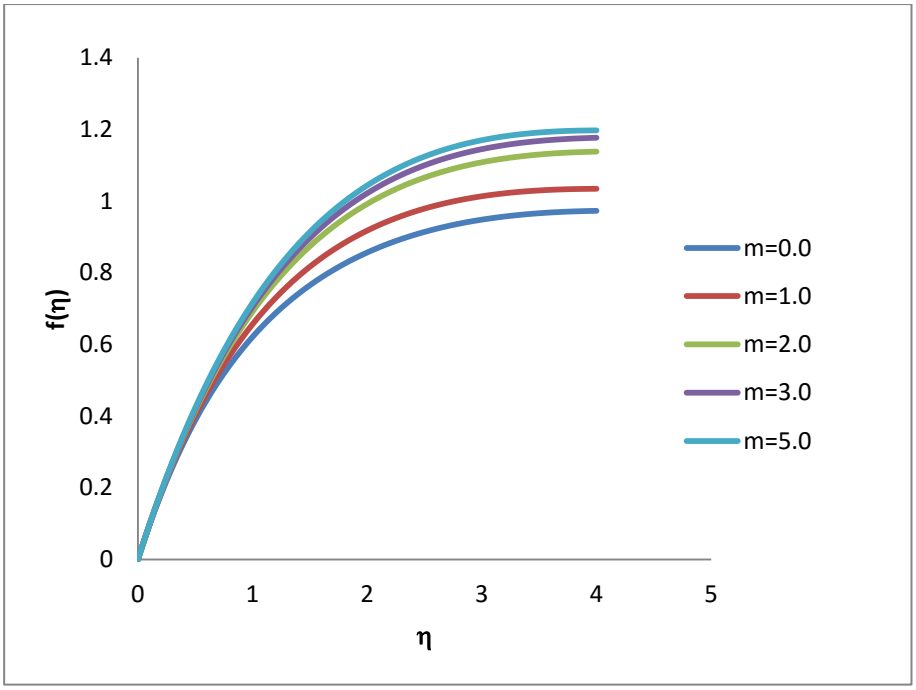

Fig 4.8 Transverse velocity of $f(\eta)$ for various values of Hall Current parameter m; Pr=7.0; Sc=0.5; Sr=0.5; Gr=0.5; Gc=0.5; k=0.2; M=1.0*

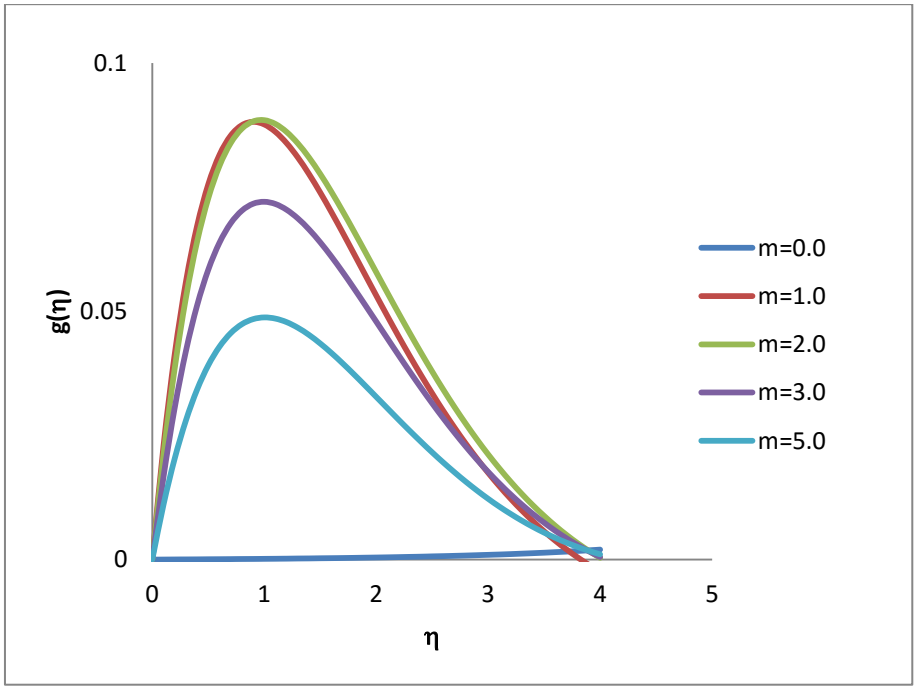

Fig 4.9 Cross flow velocity of $g(\eta)$ for various values of Hall Current m; Pr=7.0; Sc=0.5; Sr=0.5; Gr=0.5; Gc=0.5; k=0.2; M=1.0*

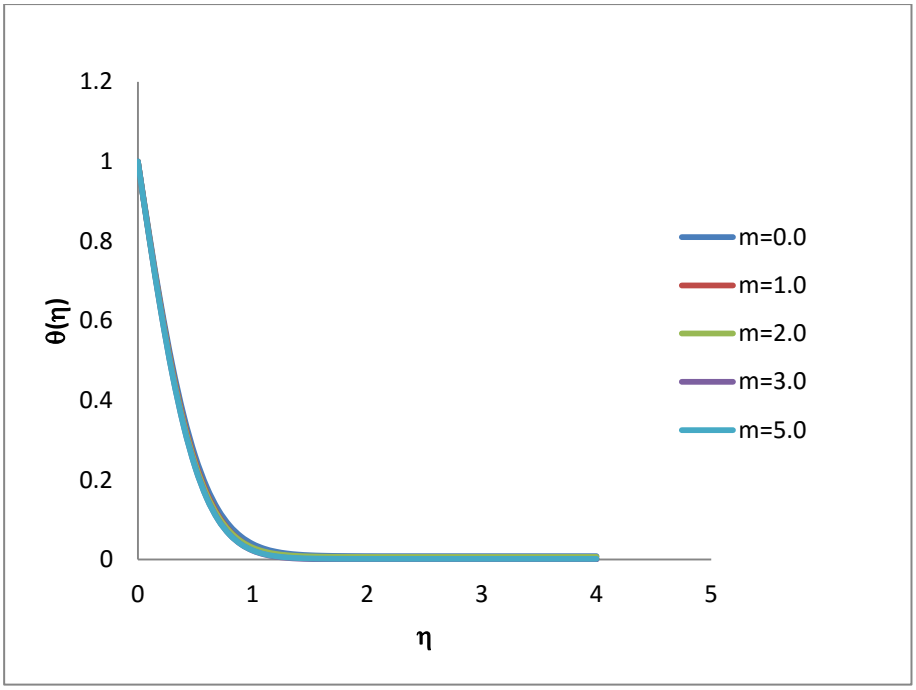

Fig 4.10 Temperature profiles of $\theta(\eta)$ for various values of Hall Current parameter m; Pr=7.0; Sc=0.5; Sr=0.5; Gr=0.5; Gc=0.5; k=0.2; M=1.0*

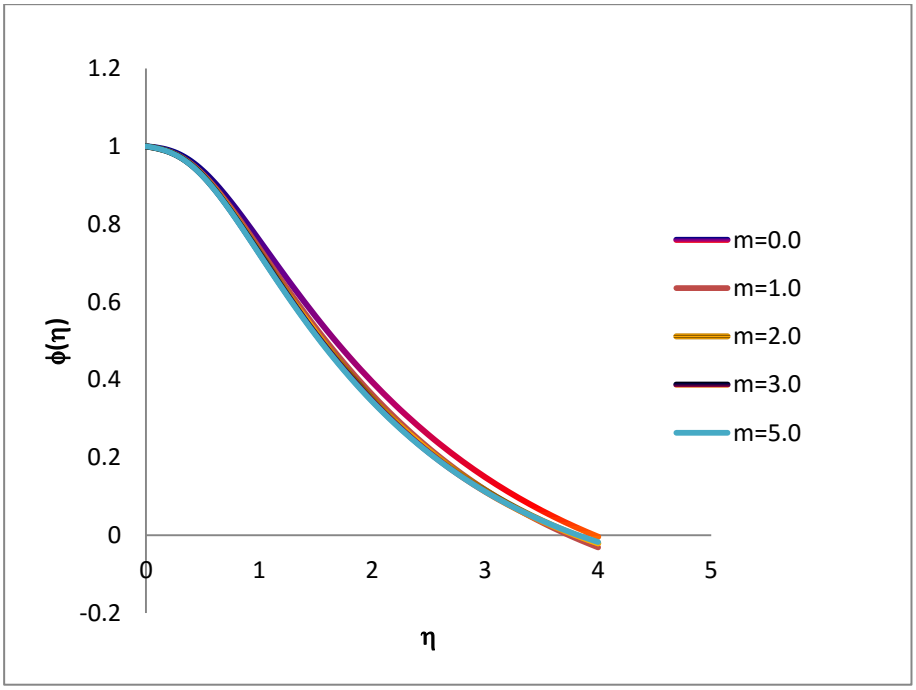

Fig 4.11 Concentration profiles $\phi(\eta)$ for various values Hall Current parameter m; Pr=7.0; Sc=0.5; Sr=0.5; Gr=0.5; Gc=0.5;k=0.2; M=1.0*

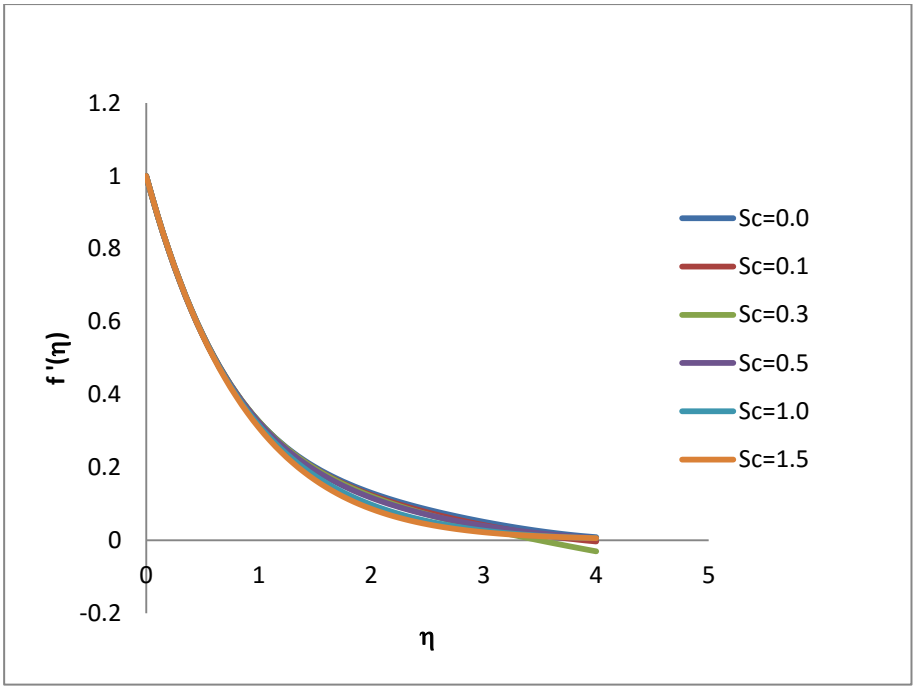

Fig 4.12 Axial velocity of $f'(\eta)$ for various values of Sc; Pr=7.0; Sr=0.5; Gr=0.5; Gc=0.5; k=0.2; M=2.0; m=1.0*

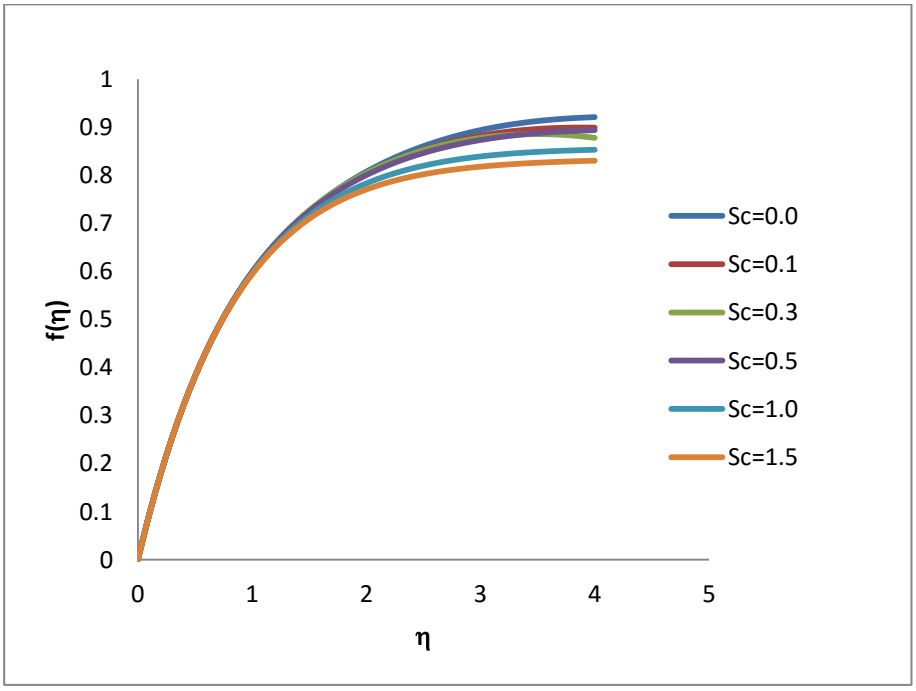

Fig 4.13 Transverse velocity of $f(\eta)$ for various values of Sc; Pr=7.0; Sr=0.5; Gr=0.5; Gc=0.5; k=0.2; M=2.0; m=1.0*

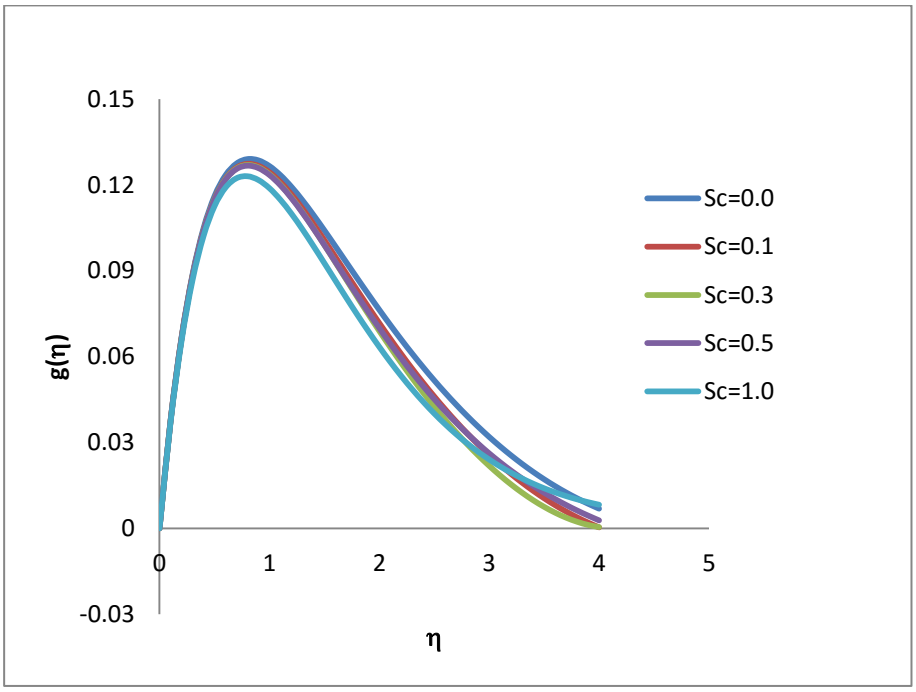

Fig 4.14 Cross flow velocity of $g(\eta)$ for various values of Sc; Pr=7.0; Sr=0.5; Gr=0.5; Gc=0.5; k=0.2; M=2.0; m=1.0*

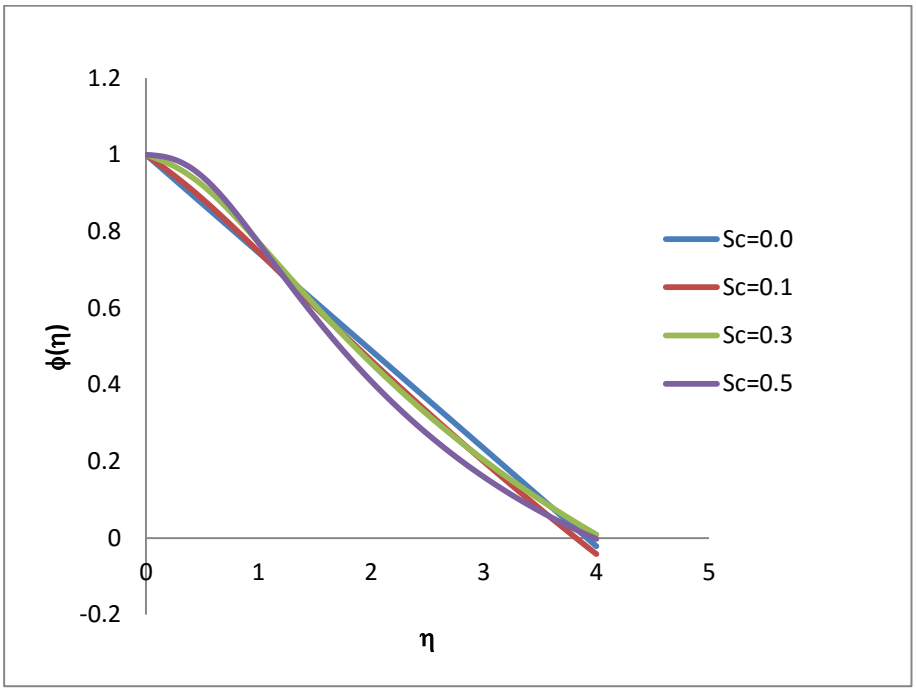

Fig 4.15 Concentration profiles $\phi(\eta)$ for various values of Sc; Pr=7.0; Sr=0.5; Gr=0.5; Gc=0.5; k=0.2; M=2.0; m=1.0*

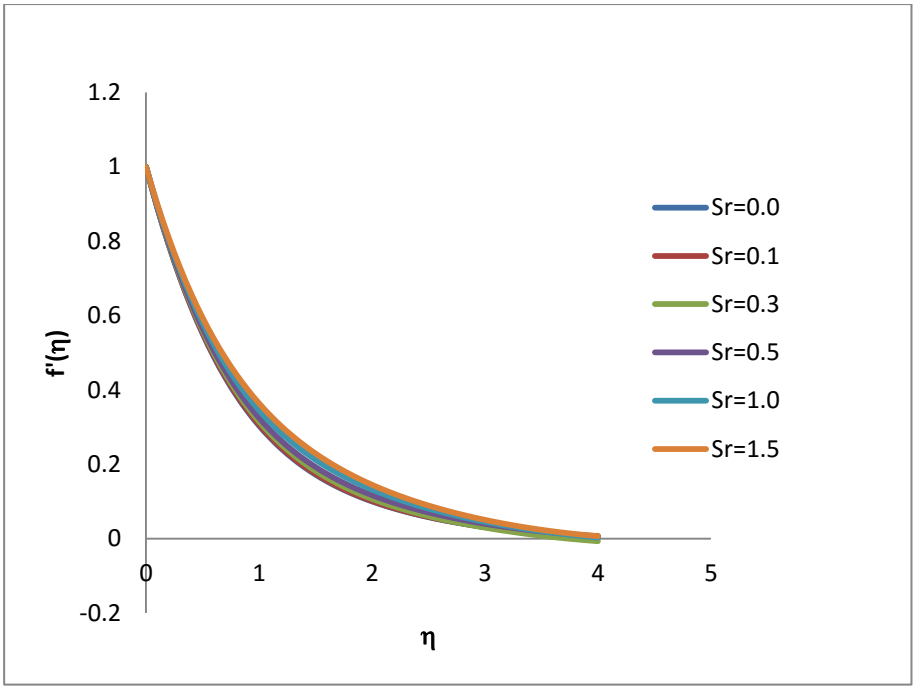

Fig 4.16 Axial velocity of $f'(\eta)$ for various values of Sr; Pr=7.0; Sc=0.5; Gr=0.5; Gc=0.5; k=0.2; M=2.0; m=1.0*

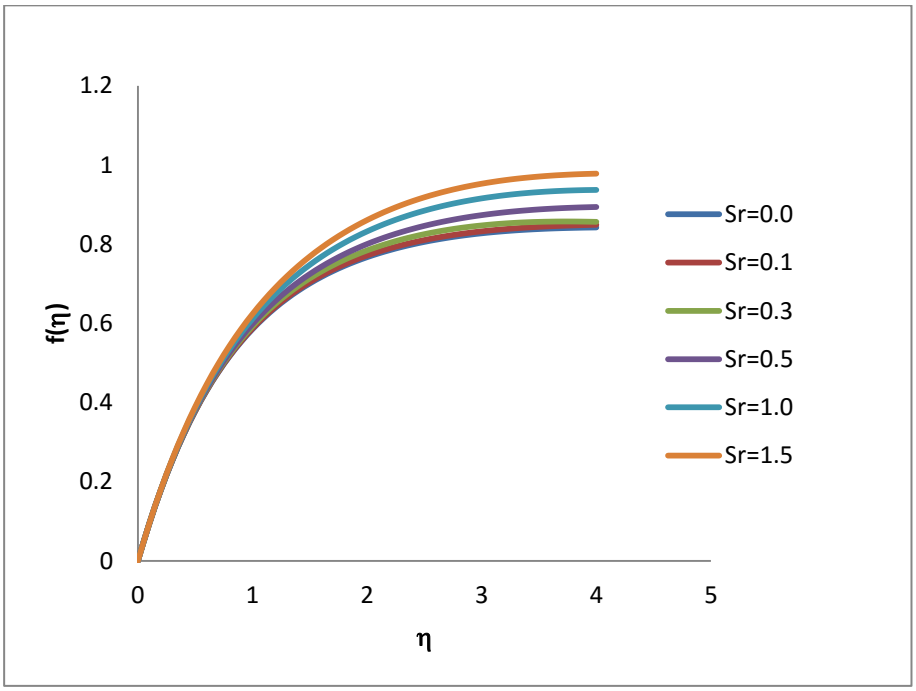

Fig 4.17 Transverse velocity of $f(\eta)$ for various values of Sr; Pr=7.0; Sc=0.5; Gr=0.5; Gc=0.5; k=0.2; M=2.0; m=1.0*

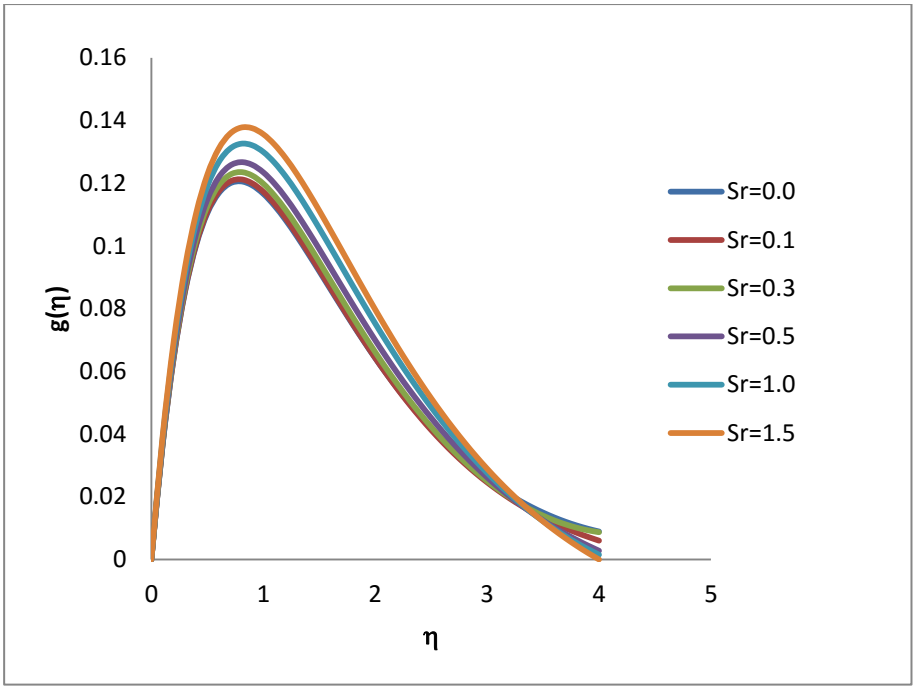

Fig 4.18 Cross flow velocity of $g(\eta)$ for various values of Sr; Pr=7.0; Sc=0.5; Gr=0.5; Gc=0.5; k=0.2; M=2.0; m=1.0*

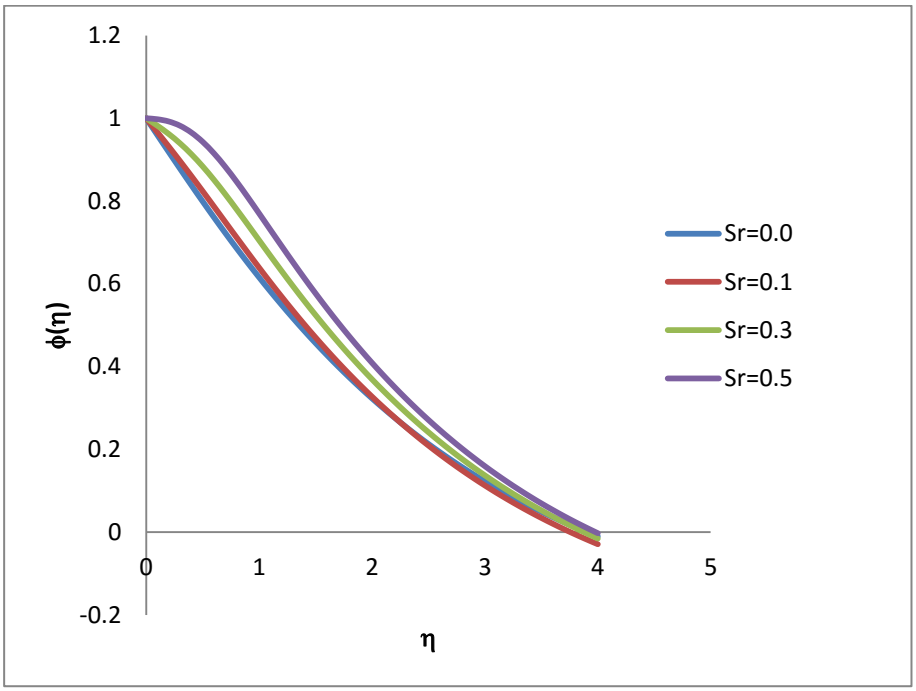

Fig 4.19 Concentration profiles $\phi(\eta)$ for various values of Sr; Pr=7.0; Sc=0.5; Gr=0.5; Gc=0.5; k=0.2; M=2.0; m=1.0*

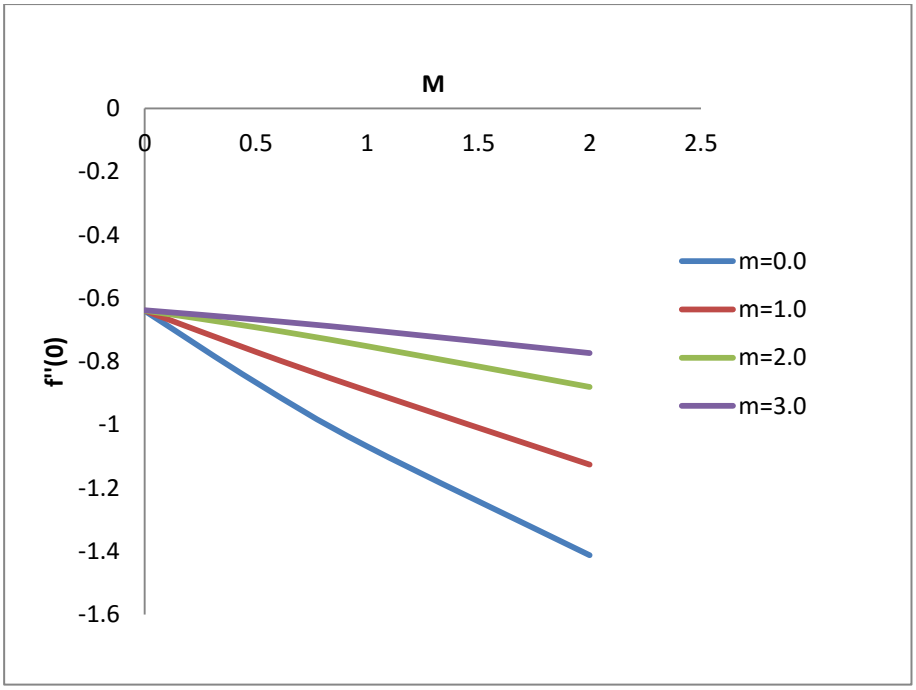

Fig 4.20 Skin-friction coefficient $f''(0)$ against magnetic parameter M for various values of Hall current parameter m; Pr=7.0; Sc=0.5; Sr=0.5; Gr=0.5; Gc=0.5; k=0.2*

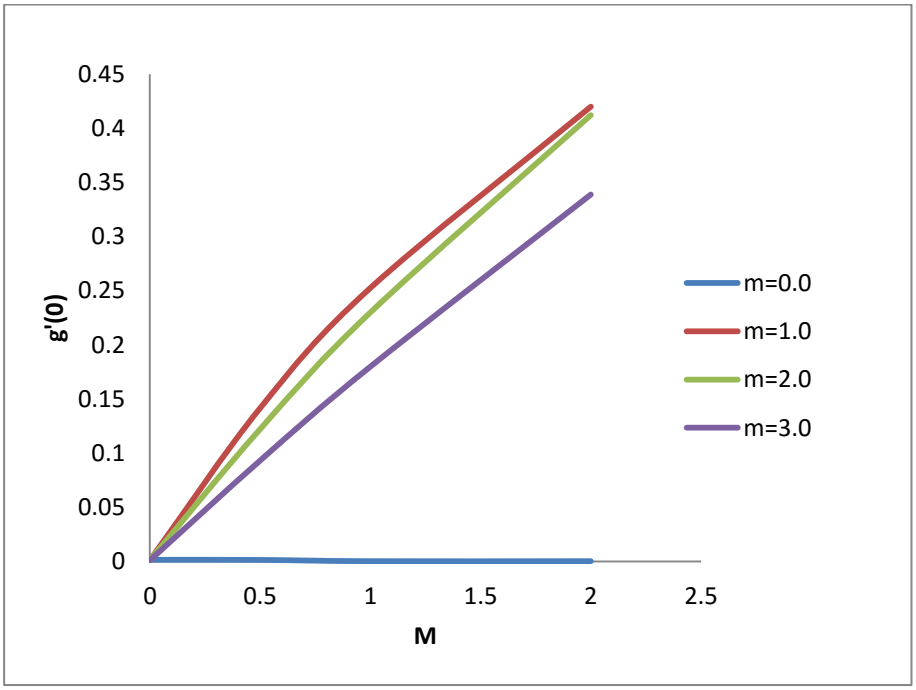

Fig 4.21 Shear stress in z-direction $g'(0)$ against magnetic parameter M for various values of Hall current parameter m; Pr=7.0; Sc=0.5; Sr=0.5; Gr=0.5; Gc=0.5; k=0.2*

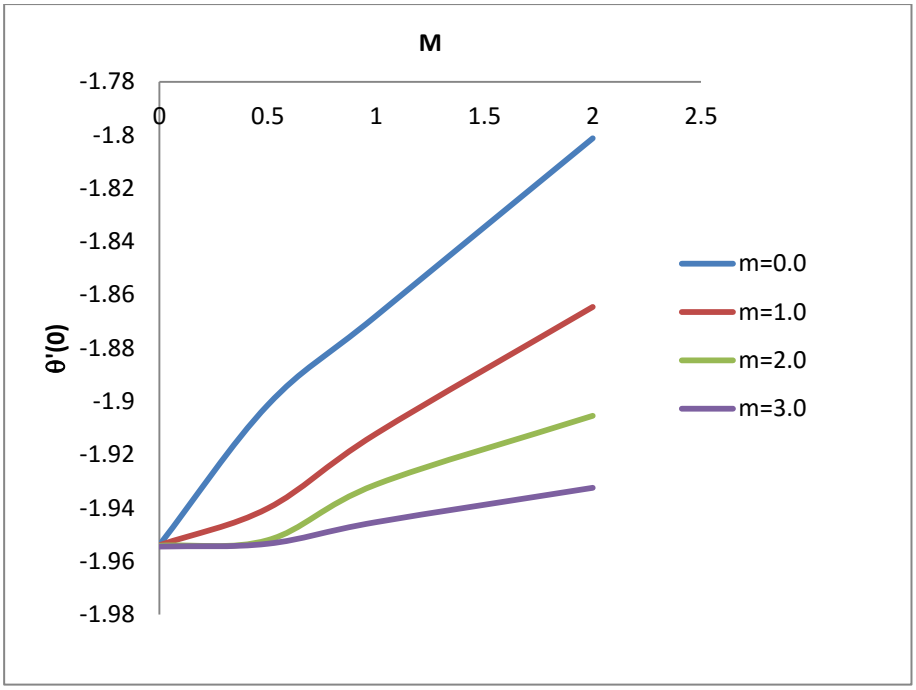

Fig 4.22 Rate of heat transfer at the plate $\theta'(0)$ against magnetic parameter M for various values of Hall current parameter m; Pr=7.0; Sc=0.5; Sr=0.5; Gr=0.5; Gc=0.5; k=0.2*

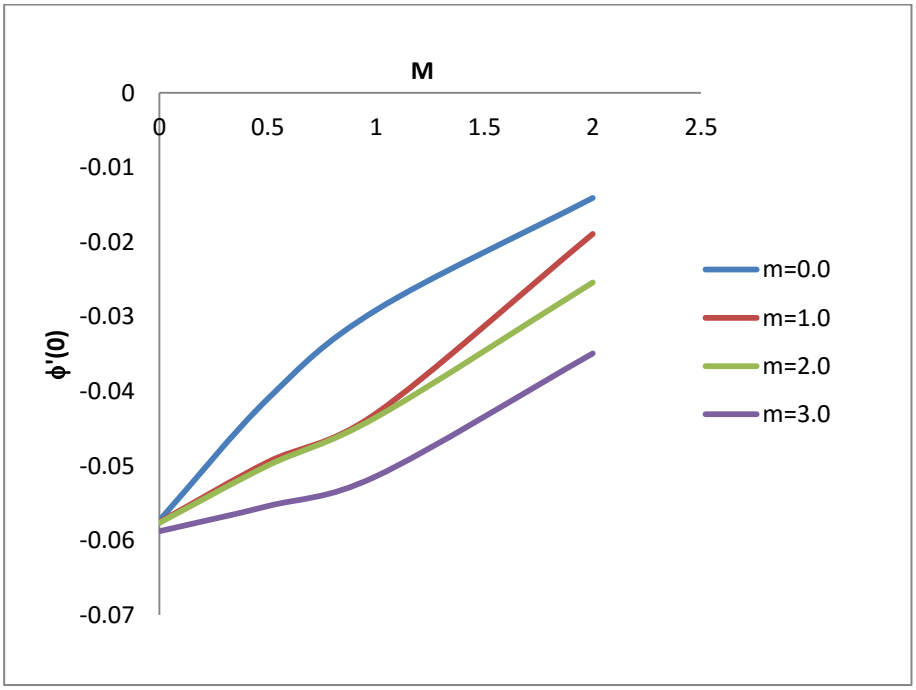

Fig 4.23 Rate of mass transfer at the plate $\phi'(0)$ against magnetic parameter M for various values of Hall current parameter m; Pr=7.0; Sc=0.5; Sr=0.5; Gr=0.5; Gc=0.5;k=0.2*